Kurdistan Journal of Applied Research (KJAR)
Print-ISSN: 2411-7684 | Electronic-ISSN: 2411-7706

Website: Kjar.spu.edu.iq | Email: kjar@spu.edu.iq

Kidney Diseases Classification using Hybrid Transfer-Learning DenseNet201-Based and Random Forest Classifier

Abdalbasit Mohammed Qadir
Computer Science
College of Science and Technology
University of Human Development
Sulaimani, Iraq
Abdalbasit.mohammed@uhd.edu.iq

Dana Faiq Abd
Computer Science
College of Science and Technology
University of Human Development
Sulaimani, Iraq
Dana.abd@uhd.edu.iq

Article Info

Volume 7 – Issue 2- December 2022

DOI: 10.24017/Science.2022.2.11

Article history:

Received: 23/09/2022
Accepted: 04/01/2023

Keywords:

Kidney Disease, AI-Based System, Machine Learning, Pre-Trained Model, Feature Extraction, Classification

ABSTRACT

There are several disease kinds in global populations that may be related to human lifestyles, social, genetic, economic, and other factors related to the nature of the country they live in. Most of the recent studies have focused on investigating prevalent diseases that spread in the population in order to minimize mortality risks, choose the best method for treatment, and improve community healthcare. Kidney disease is one of the most widespread health problems in modern society. This study focuses on kidney stones, cysts, and tumors, the three most common types of renal illness, using a dataset of 12,446 CT urogram and whole abdomen images Available: https://www.kaggle.com/nazmul0087/ct-kidney-dataset -normal-cyst-tumor-and-stone, aiming to move toward an AI-based kidney disease diagnosis system while contributing to the wider field of artificial intelligence research. In this study, a hybrid technique is used by utilizing both pre-trained models for feature extraction and classification using machine learning algorithms for the task of kidney disease image diagnosis. The pre-trained model used in this study is the Densenet-201 model. As well as using Random Forest for classification, the Densenet-201-Random-Forest approach has outperformed many of the previous models used in other studies, having an accuracy rate of 99.44 percent.

1. INTRODUCTION

The spread of kidney disease, despite many restrictions and preventions to contain it, is a public health concern [1]. Studies show that more than 10% of people worldwide have chronic renal disease [2], and it was listed as the 16th largest cause of death in 2016; by 2040, it is anticipated to move up to the 5th spot [3]. The most common kidney diseases that impair kidney function are renal cell carcinoma (kidney tumor), cyst development, and nephrolithiasis (kidney stones). A fluid-filled pocket with a thin wall that develops on the surface of the kidney is called a kidney cyst. One or more cysts with water density may form inside the kidneys, ranging from 0 to 20 units of Hounsfield [4-6]. Approximately 12% of the world's population suffers from the kidney condition known as “stone disease” in the kidneys, which is formed when the kidneys inside start to develop crystal concretions [7]. One of the ten diseases with the highest incidence rates in the world is kidney tumor which is scientifically known as renal cell carcinoma (RCC) [8].

A report was published in 2017 [9] that estimated the overall number of deaths related to kidney diseases worldwide from 1990 to 2017. According to the report, more than 130 thousand people die annually on average worldwide. The report also showed that the estimated number of deaths in 2017 was around 10 million. It was almost 17 percent of all deaths in that year. Moreover, smoking, diabetes, obesity, heart disease, hypertension, a family history of kidney disease, drug, alcohol abuse, overdose, drugs, sex, age, urinary function changes, difficulty during urination, vomiting, blood in the urine, nausea, flank pain, metallic taste, drowsiness, ammonia breath, inattention, chills, rash, and shortness of breath are all symptoms of kidney disease [10] bone disease, High blood pressure, anemia, and cardiovascular disease are all possible outcomes of this condition.

In order to detect kidney disease, many techniques and screening ways are used alongside with pathology tests such as X-ray, MRI (magnetic resonance imaging), computed tomography (CT), and B-ultrasound machines. By using X-ray beams, the CT machine, a cross-sectional picture is produced through scanning a targeted area of the human body. This technique can be used to reconstruct the desired area in three dimensions [11]. CT scans of the kidneys are great for research because they give both slice-by-slice pictures and three-dimensional data. A late diagnosis of kidney problems such as stones, cysts, and tumors can lead to renal failure. That's why it seems logical that identifying kidney problems like cysts, stones, and tumors as early as possible would be beneficial in warding off kidney failure.

But there is a severe shortage of urologists, radiologists, and other specialists. One nephrologist serves a population of a million in South Asia, whereas the corresponding figure for Europe is 25.3. With so many people in need of help, so few nephrologists and radiologists available, and with deep learning research making great strides in vision tasks, it is time for us to create an AI that can diagnose and treat kidney disease [12]. For the sake of patient care and medical progress, it is critical that a model for detecting renal radiological abnormalities be developed. There has only been a few of research published in this area in the last several years. However, there is a lack of data that is freely accessible to the public. Furthermore, the vast majority of previous research has only used conventional machine learning algorithms to categorize a specific kind of disease, such as cysts, tumors, or kidney stones. Ultrasound (US) imaging has been used in a few research projects.

For this study, we have worked on the dataset named “CT KIDNEY DATASET: Normal-Cyst-Tumor and Stone” and implemented a hybrid model consisting of the Densenet-201 pre-trained model and using it for feature extraction while using random forest algorithm for the classification of the CT-Radiography images, and evaluated the model. The suggested auto-detection methodology for kidney disease diagnostics used in this study can aid in creating a digital twin of renal function in the context of pathology. This study has bypassed the other studies' performance and contributes greatly to the medical field, specifically for kidney disease detection [13].

2. RELATED WORK

Md Nazmul et.al. [13] worked on developing an AI-based system for diagnosing kidney disease and contributed to the AI community's research efforts. This study focuses on the three main categories of renal diseases: cysts, tumor, and kidney stones. Experimenting with the gathered photographs' data showed a similarity in the mean color distribution across all categories. In addition, this research used six machine learning models, in which three of these modules were pre-trained models based on transfer learning, which are Resnet, VGG16, and Inception v3, with some minor adjustments made in the final layers of each, and the other three were based on the most recent versions of the Vision transformers (Swin transformers, EANet, and CCT). The swin transformer had a 99.30 percent accuracy rate, which was much higher than that of the VGG16 and CCT models. In both speed of training and accuracy, the Swin transformer is shown to be the best option. Their investigation of VGG16, Inception, and Resnet50, showed that VGG16 is the best model for keeping an eye on crucial anatomical irregularities, whereas Resnet50 and Inceptionv3 fell short. This research demonstrates that both the VGG16-based model and the Swin transformer model can provide benefit in the diagnosis of kidney tumor, cysts, and stones because of their higher accuracy.

Enes et.al. [14] focused on identifying the most important predictors of early kidney disease diagnosis, with the goal of facilitating earlier patient treatment and avoiding consequences. Diagnosis and prognosis were the focus of their research, which used data from 150 healthy individuals and 250 people with chronic kidney disease in order to draw conclusions. Training and test data for patients with chronic renal disease were first categorized using machine learning algorithms. Consistent information and research were used to evaluate the Chronic Renal Disease estimate outcomes.

S. Vijayarani et.al. [15] The purpose of this study is to use artificial neural networks and support vector machines (SVM) in order to foretell renal disorders. The focus of this study is to evaluate these two algorithms side-by-side in terms of their speed and precision. The experimental findings show that the ANN outperforms the competing method.

Daniel et.al. [16] stated that in order to aid in detection and minimize effort, algorithms based on deep learning that use abdominal noncontrast CT images might be useful. They were the first to work on a dataset in terms of scale and test such a system, while using it on noisy low-dose CT. The method improved upon a previous study that acquired a sensitivity of 0.52 by achieving 0.5 false positives per scan with a test set sensitivity of 0.86 on low dose CT with numerous tiny stones.

Kristian et.al. [17] worked on a multi-class classification model using a CNN pre-trained model, named ResNet-101. Leave-one-out cross validation was used on the model for evaluation. The results showed that the composition prediction recall ranged from 94 percent (n=17) for uranium acetate to 71 percent (n=14) for chromium hydride phosphate dihydrate (CHPD) and brushite. As a whole, the model’s composition analysis had an 85% weighted recall. The results for the various types of stones were as follows in terms of specificity and accuracy: COM [97.62, 95], UA [97.83, 94.12], cystine [98.31, 75], struvite [91.84, 71.43], and brushite [96.43, 75].

A. Nithya et.al. [18] in their research, they suggested an artificial neural network for detecting kidney stones, and a k-means clustering multi-kernel approach for segmenting them. They use a median filter to primarily get rid of any noise in the input picture. Then, the image's crucial GLCM characteristics were retrieved. Following that, a neural network classifier is used to determine whether or not the picture is normal. The aberrant photos are then passed on to the step of segmentation, where a multi-Kernel K-means clustering technique is utilized to detect tumor parts and the stone. The experimental findings demonstrate that, in comparison to other approaches, the suggested system provides the highest accuracy, at 99.61 percent.

Jyoti et.al. [19] The researchers in this work began by using the Gaussian filter, median filter, and un-sharp masking to improve the quality of the images. Then, they performed morphological processes like erosion and dilation to prepare the pictures for analysis; next,

entropy-based segmentation was used in order to locate the area of interest; and lastly, they used KNN and SVM classification strategies for the process of classifying the stones.

Kadir et.al. [20] in this article, an automatic kidney stone (stone presence/absence) identification method employing coronal computed tomography (CT) images and deep learning (DL) technology is proposed, which has lately made major strides in artificial intelligence. Taking unique cross-sectional CT pictures of each individual yielded a total of 1,799 images. Using CT scans to identify kidney stones, their automated model had an accuracy of 96.82 percent. They have discovered that their model can properly identify kidney stones of even the smallest size. With a bigger dataset of 433 participants, their DL model produced higher results and is suitable for clinical use. This work demonstrates that the increasingly popular DL approaches may be used for other difficult situations in urology.

Maha et.al. [21] this review article reviews the research on radiology imaging related to deep learning and summarizes the scientific progress that has been achieved, as well as determining the ways and techniques that researchers have used in the previous years in order to diagnose kidney tumors from medical images and identify future avenues, whether in terms of technological developments or applications.

Abubaker et.al. [22] the authors of this article, addressed recent advancements in DL-based kidney tumor segmentation systems. They address the many kinds of medical imaging and segmentation methodologies, as well as the evaluation criteria for segmentation results in the segmentation of kidney tumors, emphasizing their constituent parts and tactics.

Sudharson et.al. [23] proposed the use of transfer learning for the automatic classification of B-mode kidney from patient ultrasound images through the use of an ensemble of deep neural networks (DNNs). In this study, different pretrained DNNs like MobileNet-v2, ResNet-101, and ShuffleNet are combined to produce the final prediction using the majority voting technique. Instead of using individual models, better classification performance is observed when predictions from multiple DNNs are ensembled. The model used in this study categorized the kidney ultrasound images into four classes: stone, tumor, normal, and cyst. On noisy images, a classification accuracy of 95.58% was achieved, while in the testing with quality images, the model's accuracy reached 96.54%.

Dalia et.al [24] collected 8,400 images of 120 adult patients from the King Abdullah University Hospital (KAUH) from patients who performed CT scans on which they were suspicious of having kidney masses. For the classification process, authors used three models, namely, ResNet50 with 50 layers, a 2D convolutional neural network with six layers (CNN), and VGG16 with 16 layers. In the experiments, an accuracy of 96%, 97%, and 60% was achieved, respectively, for each model.

3. METHODOLOGY

This section provides a full overview of the technique used. Figure 1 depicts the proposed Kidney Cyst, Stone, and Tumor Detection system, which uses the "Densely Connected Convolutional Neural Network" (DenseNet-201) for feature extraction and random forest classifier for classification.

The design of the proposed model comprises three stages: preprocessing, feature extraction, and classification.

3.1 The pre-processing Stage

In the majority of image classification applications, utilizing a pre-trained convolutional neural network is intended to reduce the computational complexity of the model, which is likely to grow when the inputs are images. In this study, the original 3-channel pictures were reduced from various image sizes to 224x224 pixels in order to minimize computational load and increase processing speed. All subsequent procedures have been applied to these reduced photos.

3.2 The feature extraction stage

In this work, a Deep Transfer Learning model of DenseNet201 is proposed for feature extraction. Using its own learned weights and a random forest classifier for the classification phase, the proposed model collects features from the dataset. The architecture of DenseNet201 is shown below.

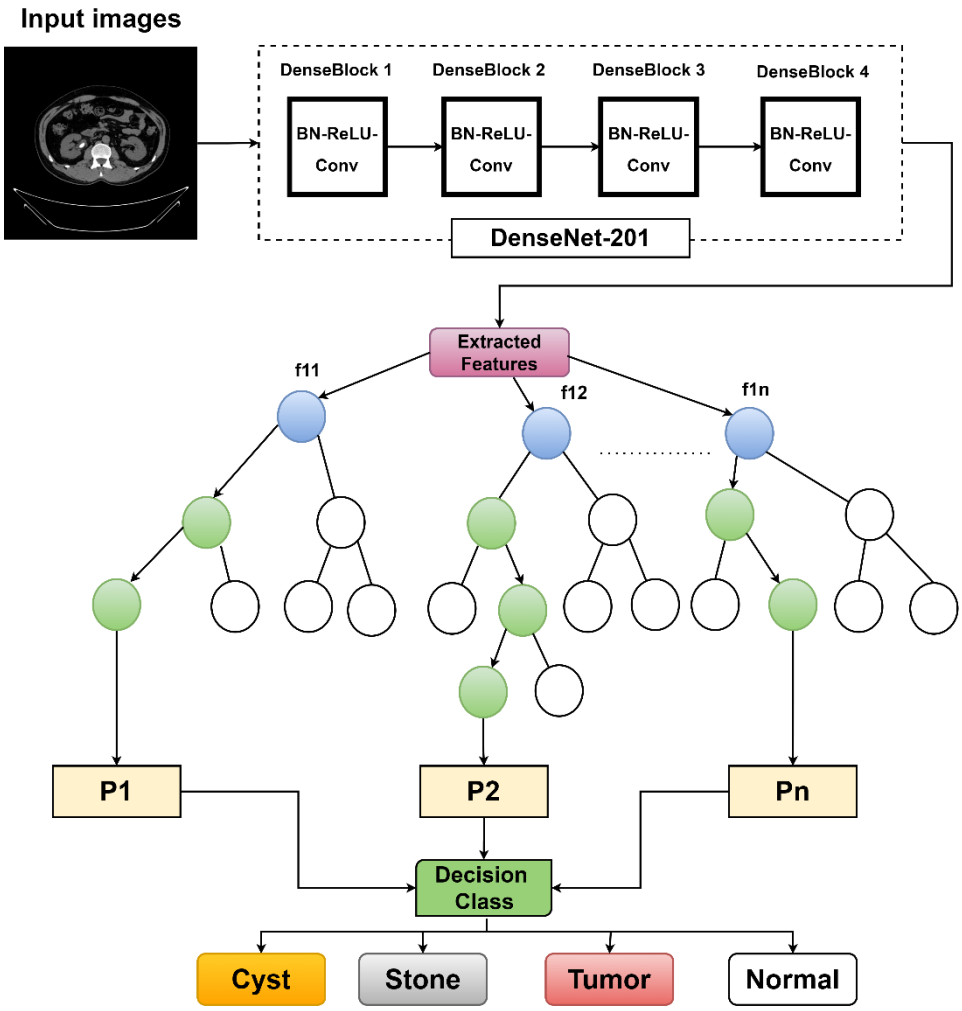

Figure 1: Densenet-201-Random Forest Architecture

The DenseNet201 makes use of the condensed network to produce models that are simple to train and extremely parametrically efficient owing to the potential of feature reuse by successive layers, This increases the diversity of the subsequent layer's input and improves the performance of the model [25]. On several datasets, including ImageNet and CIFAR-100, the DenseNet201 shown remarkable performance. To boost connectivity in the DenseNet201 model, as seen in figure 2, direct connections are made from all preceding levels to all succeeding layers. Mathematically, the feature concatenation may be described as:

$$z^{l} = H_{l}([z^{0}, z^{1}, \dots\dots, z^{l-1}]) \qquad (1)$$

Here, H_l is a nonlinear transformation that may be written as a composite function consisting of batch normalization (BN), a rectified linear unit function (ReLU), and a convolution of linear unit functions (3 x 3). $[z^0, z^1, \ldots\ldots, z^{l-1}]$ refers to the concatenation of feature maps corresponding to layer 0 to $l-1$. They are combined into a single tensor to facilitate implementation. For the purpose of down sampling, dense blocks are created in the network architecture and separated by BN transition layers, 1 x 1 convolution, and 2 x 2 average pooling. The DenseNet201 growth rate, denoted by the hyperparameter k, demonstrates how the dense design produces state-of-the-art outcomes. Due to its design, which considers feature maps as the global state of the network, DenseNet201 functions adequately even with a lower growth rate. Consequently, each following layer has access to each preceding layer's feature maps.

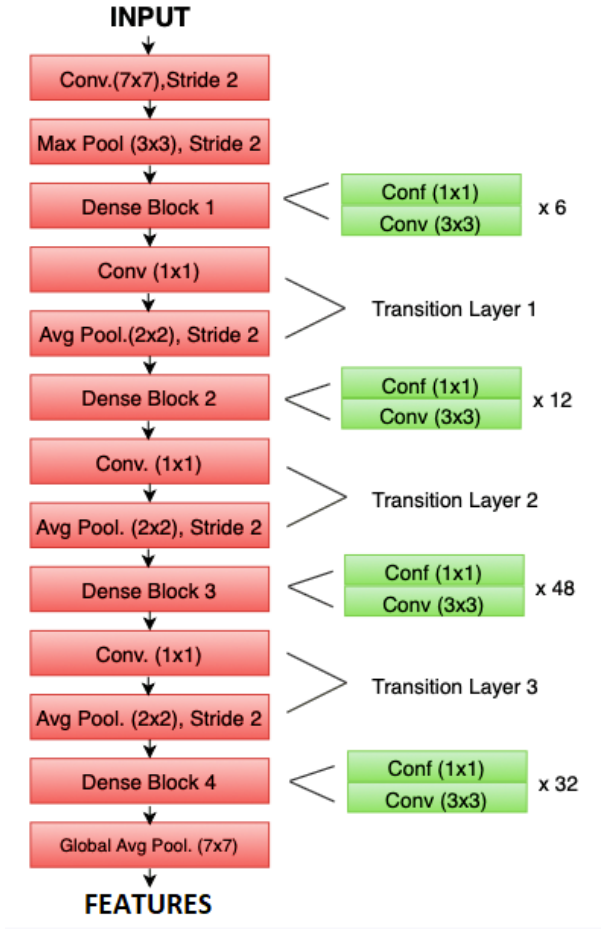

Figure 2: Densnet-201 Architecture

Each layer provides k feature maps to the global state, where k is more than the total number of input feature maps at the I^{th} layer $(FM)^I$ is calculated as follows:

$$(FM)^l = k^0 + k(l-1) \quad (2)$$

Here, k^0 defines the input layer's channels. Every 3x3 convolution layer is preceded by a 1x1 convolution layer, which minimizes the number of input feature maps, which are often more than the output feature map count, k. The added 1x1 convolution layer yields 4k feature maps and is referred to as the bottleneck layer.

3.3 The classification stage using Random Forest

The third phase of our proposed model after preprocessing and feature extraction is classification based on the extracted features from the DenseNet201 model. In this phase, Random Forest algorithm is used which is one of the most widely used and efficient ensemble learning techniques, especially for high-dimensional classification and skewed problems. Achieving very good performance in machine learning and pattern recognition, it has been shown to be quite popular and successful. But variability is one of the disadvantages of tree classifiers. In fact, sometimes a little change in the data of the training set might lead to a radically different tree. This is because tree classifiers are hierarchical. If there was an error in a node that is close to the tree's root, then this error will extend to every leaf. The goal of random forest is to create a reliable tree classification, for which a decision forest approach has been developed. A decision forest consists of many decision trees. It can be viewed as a single or several classification methods belonging to a classifier or as an individual method with multiple work parameters. Consider a learning set L = ((M1, N1), . . ., (Mn, Nn)) classifier for classification issues is a mapping X→Y [26]. Each unique tree inside the forest classifies a new vector input. Each tree produces a distinct categorization outcome. The classification with the majority of the votes among all the trees is chosen by the decision forest. The technique of this classifier includes Breiman's [27] The concept of "bagging" and "random selection". Bagging, which means "bootstrap aggregation," is an ensemble learning type which is developed by Breiman to enhance the accuracy of a poor classifier generating several classifiers in a dataset if N is the number of occurrences, approximately two-thirds of the original size is picked at random N times using the bootstrapping method. The remaining occurrences have been analyzed using an out-of-bag set which contains data that was not used to build the subtrees. This is also useful for the prediction of error rates. Using a random selection of characteristics, a decision node is formed at each node. At each split, the feature size is $\sqrt{m}\ or\ \sqrt{m}\ /2$ where m is the number of features [28]. Since no pruning is done, all of the sub-trees are maximum trees.

On each decision tree, random forest training is conducted. In this method, the training set of each classifier is built by randomly picking N samples with replacement, where the training set size is N. The samples are used to develop a classifier, and from the trials, these classifiers are combined to produce the main classifier. To categorize a situation, the instance is allocated to the class with the highest votes. In the case that several classes majority votes are equal, the winner is selected randomly. From the input data, an independently drawn bootstrap copy of the data is assigned to each tree in the classifier [29]. Based on its out-of-bag observations, the process is ensemble error prediction is performed from the forecasts for each tree, as well as calculating the averaging of these predictions throughout the whole ensemble. This is applied to every single observation, and then equates the expected out-of-bag response at this observation to its actual value. The objective of bagging is to reduce the variance of a learner with no inherent bias. Using this method has shown improvements in the predication ability of the ensemble since the links within the ensemble between the trees tend to be weakened by the random selection of features. To generate decision trees, RF generates a random sample of the information and recognizes a crucial arrangement of attributes. Figure 3 shows an example of the RF structure.

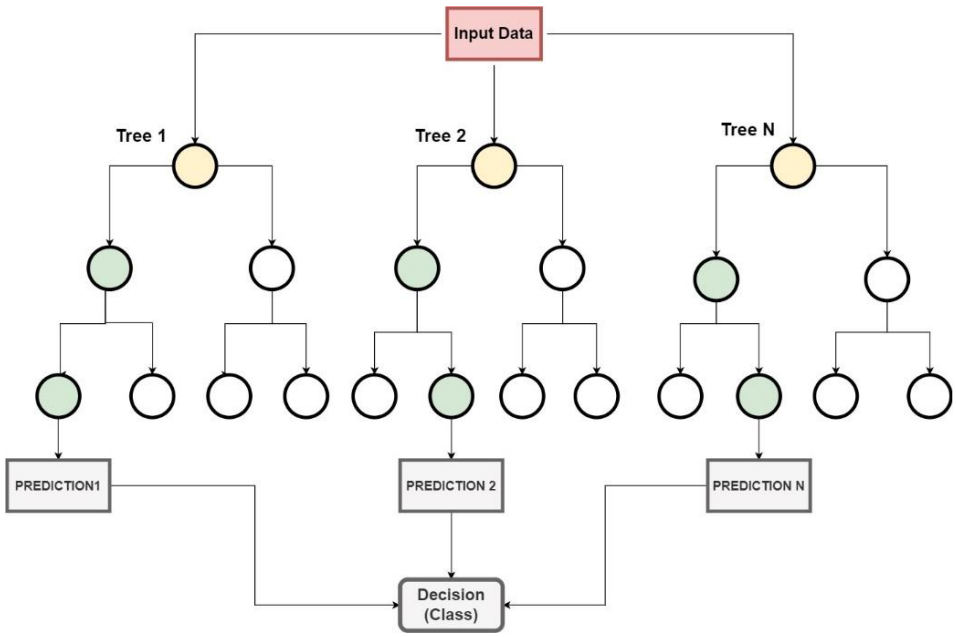

Figure 3: Random Forest Structure

4. RESULTS AND DISCUSSION

In this part, we will explain the results of the suggested kidney disease feature extraction and classification. We have used the Python language to implement the practical part of this research using the Google Colab pro service, which provides a Tesla T4 GPU to be used by researchers worldwide. Our model has been evaluated using a web-accessible data set. We have set the image size to "224x224".

4.1 Evaluation Metrics

Our model's quantitative assessment is based on the metrics of accuracy (3), precision (4), recall (5), also known as sensitivity, and F1 score (6). The total number of true positives and false negatives are divided by the number of true positives. It refers to the research's ability to appropriately identify individuals with the disease. In medical diagnostics, disorders are often classified as positive. The omission of this (positive category) has serious consequences, including misdiagnosis, which may result in patient treatment delays. Therefore, medical image diagnosis requires a high degree of sensitivity or recall. Precision (PPV) is necessary if we want to determine how many of the projected positive instances are really positive. By dividing the number of true positives by the total of true positives and false positives, precision is gained. In the field of medical imaging, accuracy is required. All models' F1 scores (6) are computed using their respective sensitivity and precision. Accuracy, precision, sensitivity, and F1 score are calculated using the following formulas:

$$Accuracy = \frac{TN + TP}{\mathrm{TN} + \mathrm{FP} + \mathrm{TP} + \mathrm{FN}} \qquad (3)$$

$$Precision = \frac{TP}{TP + FP} \qquad (4)$$

$$Recall = \frac{TP}{FN + TP} \qquad (5)$$

$$F1\ Score = 2 * \frac{Recall * Precision}{Recall + Precision} \qquad (6)$$

4.2 Dataset description

For the process of feature extraction and classification, a dataset of CT kidney images is used. which are collected in a dataset available on Kaggle under the name "CT KIDNEY DATASET: Normal-Cyst-Tumor and Stone", containing 12,446 images. The information was collected in a hospital in Dhaka, Bangladesh, using PACS (Picture Archiving and Communication System) and workstations, from individuals previously identified as having a kidney tumor, cyst, or stone. The dataset contains a total number of 12,446 unique records, of which the numbers are distributed among the classes as follows: normal has 5,077, the stone 1,379, cyst has 3,709, and the tumor 2,283.

Due to the class imbalance of the dataset, we have used the under sampling technique to solve this problem, in which we have decreased the number of image samples of the Normal, Cyst, and Tumor classes to the minimum class, which is Stone, after randomizing all the images, we have selected 1350 images from each class, which produces an even number of images for each class, thereby solving the class imbalance issue in the dataset. A detailed distribution of the dataset is provided in the following figure in terms of the number of images in each class and the under sampling technique used to balance the dataset, as well as splitting the dataset by assigning 80% of the images to the training set and 20% to the test set.

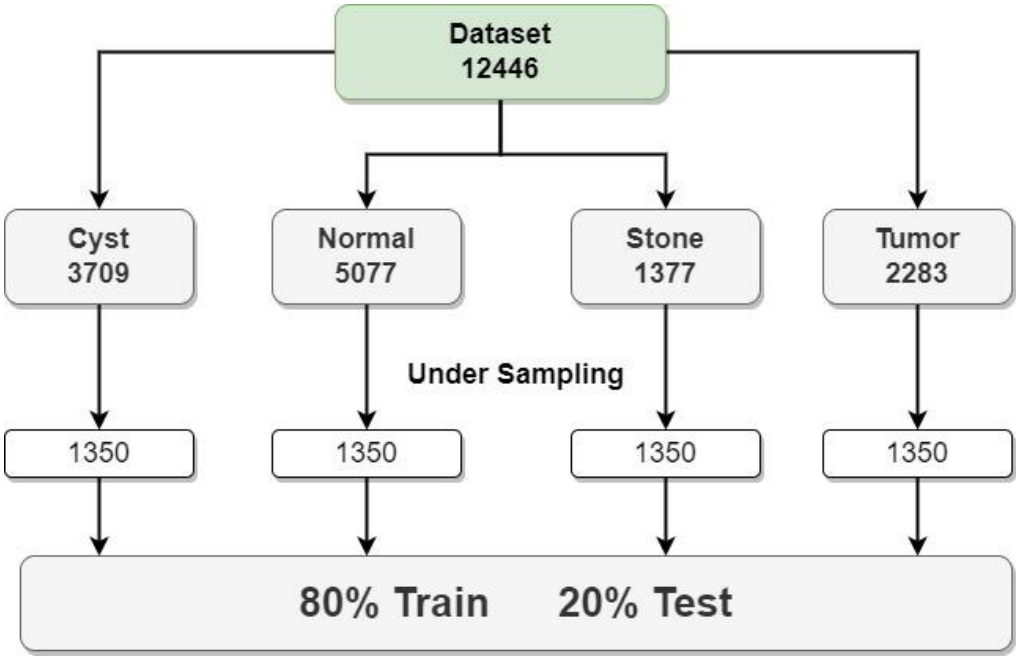

Figure 4: Dataset details

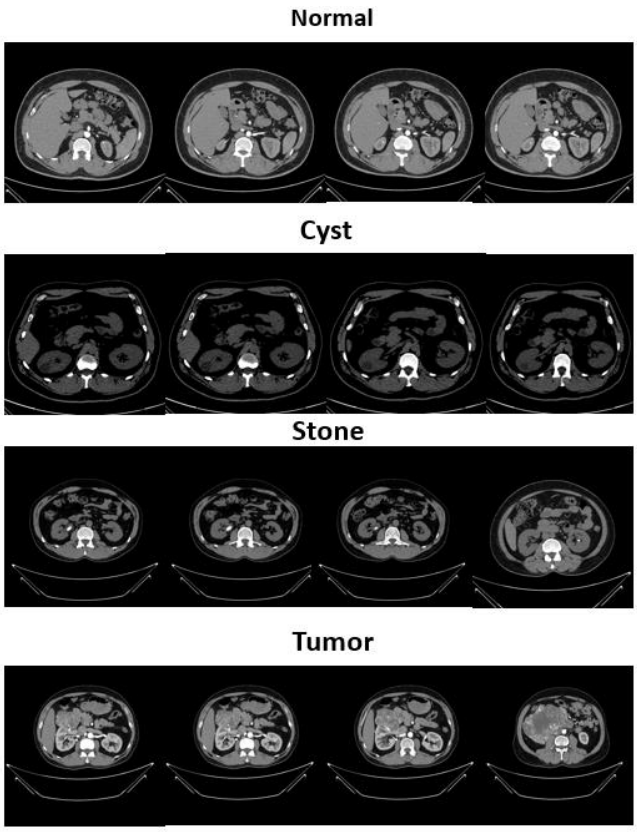

Figure 4: Image samples from the dataset

In this study, we have evaluated our proposed model using the metrics mentioned above, and we have achieved an accuracy of 99.68% on the training set and 99.44% on the test set. outperforming the other models that worked on detecting kidney diseases. The confusion matrix of our model result is shown in the following figure 6 and figure 7.

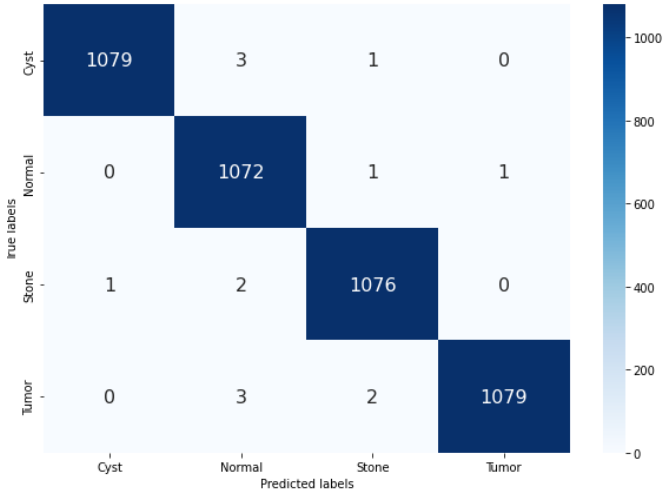

Figure 6: Training set Confusion Matrix for proposed model

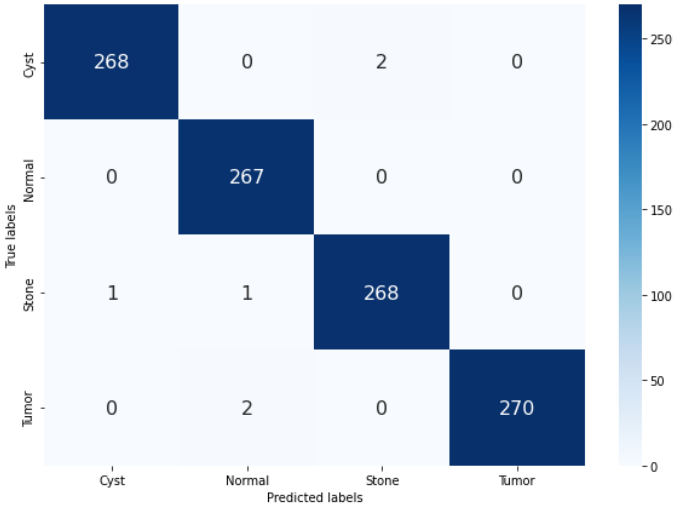

Figure 7: Testing set Confusion Matrix for proposed model

In Table 1, a comparison of the previous research on kidney disease diagnosis with our research is presented. Where our model has contributed to the field and achieved a higher performance than the other models.

Table 1: Performance metrices comparison of proposed and other models.

Study	Dataset	Model	Accuracy	Class	Precision	Recall	F1-Score
Md Nazmul et.al [13]	CT KIDNEY DATASET: Normal-Cyst-Tumor and Stone	EANET	77.02%	Cyst	0.593	1	0.745
				Normal	0.896	0.848	0.871
				Stone	0.845	0.495	0.624
				Tumor	0.93	0.777	0.847
		Swin Transformers	99.30%	Cyst	0.996	0.996	0.996
				Normal	0.996	0.981	0.988
				Stone	0.981	0.989	0.985
				Tumor	0.993	1	0.996
		CCT	96.54%	Cyst	0.968	0.923	0.945
				Normal	0.989	0.975	0.982
				Stone	0.94	1	0.969
				Tumor	0.964	0.964	0.964
		VGG16	98.20%	Cyst	0.996	0.968	0.982
				Normal	0.985	0.973	0.979
				Stone	0.966	0.988	0.977
				Tumor	0.982	0.996	0.989
		Inception V3	61.60%	Cyst	0.645	0.826	0.724
				Normal	0.584	0.898	0.708
				Stone	0.568	0.462	0.509
				Tumor	0.76	0.295	0.425
				Cyst	0.735	0.641	0.685

		Resnet50	73.80%	Normal	0.77	0.79	0.78
				Stone	0.745	0.692	0.717
				Tumor	0.706	0.827	0.762
Kadir et.al [20]	Kidney Stone Dataset	XResNet-50	96.82%	Normal	0.96	0.98	0.97
				Stone	0.98	0.96	0.97
Sudharson et.al [23]	Kidney Ultrasound Images Dataset	Ensemble DNN	96.54%	Cyst	0.96	1	0.98
				Normal	0.94	0.98	0.96
				Stone	0.97	0.90	0.94
				Tumor	0.98	0.98	0.98
Dalia et.al [24]	CT Kidney Tumors Dataset	VGG16	60%	Normal	0.57	0.90	0.7
				Tumor	0.75	0.30	0.42
		ResNet50	96%	Normal	0.98	0.95	0.96
				Tumor	0.95	0.98	0.96
		2D CNN	97%	Normal	0.96	0.97	0.97
				Tumor	0.97	0.96	0.97
Proposed Model	CT KIDNEY DATASET: Normal-Cyst-Tumor and Stone	Densenet-201-Random Forest	99.44%	Cyst	0.996	0.993	0.994
				Normal	0.989	1	0.994
				Stone	0.993	0.993	0.993
				Tumor	1	0.993	0.996

The experimental results in Table 1 show that the proposed model has a better accuracy rate than the other models, achieving 99.44 percent. The results show a 99.6% and 98.9% precision for the cyst and normal classes, respectively, and 100% for the tumor class. As for recall, the Densenet-201-Random Forest model has performed very well, with a 99.3% recall for the cyst, stone, and tumor classes, and a 100% recall for the normal class, as well as an F1-Score of 99.4% for both the cyst and normal classes. The model also performed very well in the F1-Score by achieving 99.3% and 99.6% for Stone and Tumor classes. The accuracy and error rate are visualized in Figure 8.

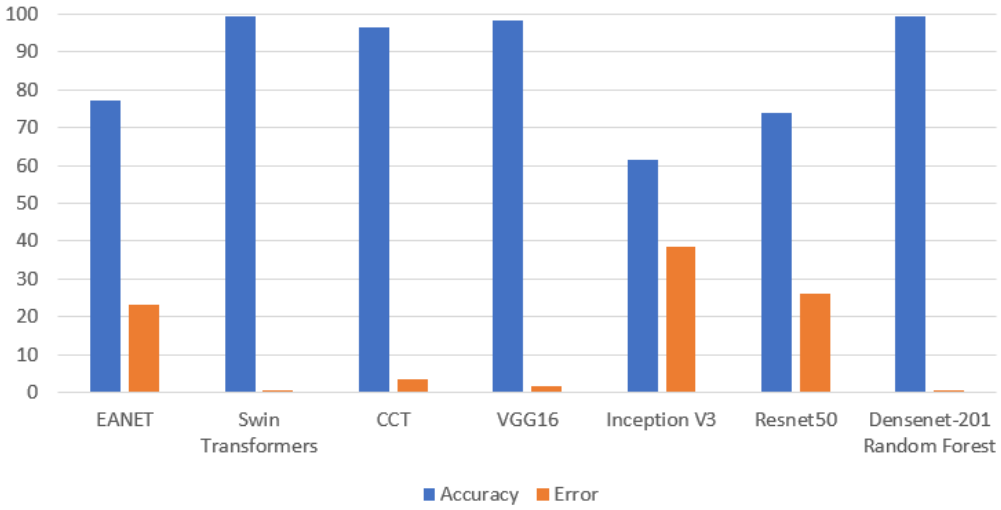

Figure 8: Accuracy/Error rate for proposed model and other models on the same dataset

5. CONCLUSION

In this work, a hybrid model was developed to extract kidney disease dataset image features and classify the images. The dataset used consists of 12,446 CT radiography images belonging to four classes, which are cysts, tumors, normal, and stone. The functionality of our model has been separated into three phases: preprocessing, in which the images were resized for less computational complexity and time reduction, feature extraction using densenet-201 and classification using Random Forest classifier. The performance of the proposed approach is evaluated using accuracy, precision, recall, and F1-score. Our model was able to achieve an accuracy of 99.44%, bypassing the other models that worked on detecting the class of kidney diseases. In order to demonstrate the efficacy of the classification stage, the suggested classifier was compared to a number of comparable research studies, and the resulting data was examined. The accuracy of our model based on DenseNet-201 and random forest classifier may lessen patients' pain and suffering by recognizing kidney tumors, cysts, and stones.

REFERENCE

[1] S. J. L. Jacobson, "Chronic kidney disease--a public health problem?," vol. 110, no. 21, pp. 1018-1020, 2013.

[2] V. Jha, *G. Garcia-Garcia, K. Iseki, Z. Li*, S. Naicker, B. Platnner, R. Saran, A. wang, C. Yang, "Chronic kidney disease: global dimension and perspectives," vol. 382, no. 9888, pp. 260-272, 2013.

[3] KJ. Foreman, N. Marquez, A. Dolgert, K. Fukutaki, N. Fullman, M. McGaughey, M. Pletcher, A. Smith, K. Tang, CW. Yuan, JC.Brown, J. Friedman, J. He, KR. Heuton, M. Holmberg, DJ. Patel, P. Reidy, A. Carter, K. Cercy, CJ. Murray, "Forecasting life expectancy, years of life lost, and all-cause and cause-specific mortality for 250 causes of death: reference and alternative scenarios for 2016–40 for 195 countries and territories," vol. 392, no. 10159, pp. 2052-2090, 2018.

[4] C. Rediger, LA. Guerra, MA. Keays, C. Wayne, D. Reddy, S. Ksara, MP. Leonard, "Renal cyst evolution in childhood: a contemporary observational study," vol. 15, no. 2, pp. 188. e1-188. e6, 2019.

[5] AJ. Brownstein, S. Mahmood, A. Saeyeldin, CV. Mejia, MA. Zafar, Y. Li, JA. Rizzo, NK. Dahl, Y. Erben, BA. Ziganshin,JA. Elefteriades, "Simple renal cysts and bovine aortic arch: markers for aortic disease," vol. 6, no. 1, p. e000862, 2019.

[6] E. Sanna , S. Loukogeorgakis , T. Prior , I. Derwig , G. Paramasivam , M. Choudhry, C. Lees, "Fetal abdominal cysts: antenatal course and postnatal outcomes," vol. 47, no. 4, pp. 418-421, 2019.

[7] T. Alelign and B. J. A. i. u. Petros, "Kidney stone disease: an update on current concepts," vol. 2018, 2018.

[8] J. Hsieh, M. Purdue, S. Signoretti, C. Swanton, L. Albiges, M. Schmidinger, D. Heng, J. Larkin, V. Ficarra, "Renal cell carcinoma," vol. 3, no. 1, pp. 1-19, 2017.

[9] S. Safiri, A. Kolahi, M. Mansournia, A. Almasi-Hashiani, A. Ashrafi-Asgarabad, M. Sullman, D. Bettampadi, M. Qorbani, M. Moradi-Lakeh, M. Ardalan, A. Mokdad, C. Fitzmaurice, "The burden of kidney cancer and its attributable risk factors in 195 countries and territories, 1990–2017," vol. 10, no. 1, pp. 1-20, 2020.

[10] S. Bala and K. Kumar, "A literature review on kidney disease prediction using data mining classification technique," 2014.

[11] K. C. Saw, J. A. McAteer, A. G. Monga, G. T. Chua, J. E. Lingeman, and J. C. J. A. J. o. R. Williams Jr, "Helical CT of urinary calculi: effect of stone composition, stone size, and scan collimation," vol. 175, no. 2, pp. 329-332, 2000.

[12] J. Sun, L. Peng, T. Li, D. Adila, Z. Zaiman, G. Melton-Meaux, N. Ingraham, E. Murray, D. Boley, S. Switzer, J. Burns, K. Huang, T. Allen, S. Steenburg, J. Gichoya, E. Kummerfeld, C. Tignanelli, "Performance of a chest radiograph ai diagnostic tool for covid-19: A prospective observational study," vol. 4, no. 4, p. e210217, 2022.

[13] M. Islam, M. Hasan, M. Hossain, M. Alam, M. Uddin, A. Soylu, "Vision transformer and explainable transfer learning models for auto detection of kidney cyst, stone and tumor from CT-radiography," vol. 12, no. 1, pp. 1-14, 2022.

[14] E. Celik, M. Atalay, A. J. I. J. o. I. S. Kondiloglu, and A. i. Engineering, "The diagnosis and estimate of chronic kidney disease using the machine learning methods," vol. 4, no. Special Issue-1, pp. 27-31, 2016.

[15] S. Vijayarani, S. Dhayanand, M. J. I. J. o. C. Phil, and B. Research, "Kidney disease prediction using SVM and ANN algorithms," vol. 6, no. 2, pp. 1-12, 2015.

[16] D. C. Elton, E. B. Turkbey, P. J. Pickhardt, and R. M. J. M. P. Summers, "A deep learning system for automated kidney stone detection and volumetric segmentation on noncontrast CT scans," vol. 49, no. 4, pp. 2545-2554, 2022.

[17] K. M. Black, H. Law, A. Aldoukhi, J. Deng, and K. R. J. B. i. Ghani, "Deep learning computer vision algorithm for detecting kidney stone composition," vol. 125, no. 6, pp. 920-924, 2020.

[18] A. Nithya, A. Appathurai, N. Venkatadri, D. Ramji, and C. A. J. M. Palagan, "Kidney disease detection and segmentation using artificial neural network and multi-kernel k-means clustering for ultrasound images," vol. 149, p. 106952, 2020.
[19] J. Verma, M. Nath, P. Tripathi, K. J. P. R. Saini, and I. Analysis, "Analysis and identification of kidney stone using Kth nearest neighbour (KNN) and support vector machine (SVM) classification techniques," vol. 27, no. 3, pp. 574-580, 2017.
[20] K. Yildirim, P. Bozdag, M. Talo, O. Yildirim, M. Karabatak, U. Acharya, "Deep learning model for automated kidney stone detection using coronal CT images," vol. 135, p. 104569, 2021.
[21] M. Gharaibeh, D. Alzu'bi, M. Abdullah, I. Hmeidi, M. Al Nasar, L. Abualigah, A. Gandomi, "Radiology imaging scans for early diagnosis of kidney tumors: a review of data analytics-based machine learning and deep learning approaches," vol. 6, no. 1, p. 29, 2022.
[22] A. Abdelrahman and S. J. J. o. I. Viriri, "Kidney Tumor Semantic Segmentation Using Deep Learning: A Survey of State-of-the-Art," vol. 8, no. 3, p. 55, 2022.
[23] S. Sudharson, P. J. C. M. Kokil, and P. i. Biomedicine, "An ensemble of deep neural networks for kidney ultrasound image classification," vol. 197, p. 105709, 2020.
[24] D. Alzu'bi, M. Abdullah, I. Hmeidi, R. AlAzab, M. Gharaibeh, M. El-Heis, K. Almotairi, A. Forestiero, A. Hussein, L. Abualigah, "Kidney Tumor Detection and Classification Based on Deep Learning Approaches: A New Dataset in CT Scans," vol. 2022, 2022.
[25] G. Huang, Z. Liu, L. Van Der Maaten, and K. Q. Weinberger, "Densely connected convolutional networks," in *Proceedings of the IEEE conference on computer vision and pattern recognition*, 2017, pp. 4700-4708.
[26] K. Fawagreh, M. M. Gaber, E. J. S. S. Elyan, and C. E. A. O. A. Journal, "Random forests: from early developments to recent advancements," vol. 2, no. 1, pp. 602-609, 2014.
[27] L. J. M. l. Breiman, "Random forests," vol. 45, no. 1, pp. 5-32, 2001.
[28] O. Okun and H. Priisalu, "Random forest for gene expression based cancer classification: overlooked issues," in *Iberian conference on pattern recognition and image analysis*, 2007, pp. 483-490: Springer.
[29] L. J. U. o. C. Breiman, Berkeley, "Bagging predictors (technical report 421)," 1994.